Protective role of podocyte autophagy against glomerular endothelial dysfunction in diabetes

Mamoru Yoshibayashi,[1] Shinji Kume,[1] Mako Yasuda-Yamahara,[1] Kosuke Yamahara,[1] Naoko Takeda,[1] Norihisa Osawa,[1] Masami Chin-Kanasaki,[1] Yuki Nakae,[2] Hideki Yokoi,[3] Masashi Mukoyama,[4] Katsuhiko Asanuma,[5] Hiroshi Maegawa,[1] and Shin-ichi Araki[1]

[1]Department of Medicine, Shiga University of Medical Science, Otsu, Shiga, Japan
[2]Departments of Stem Cell Biology and Regenerative Medicine, Shiga University of Medical Science, Otsu, Shiga, Japan
[3]Department of Nephrology, Graduate School of Medicine, Kyoto University, Kyoto, Japan
[4]Department of Nephrology, Kumamoto University Graduate School of Medical Sciences, Kumamoto, Japan
[5]Department of Nephrology, Graduate School of Medicine, Chiba University, Chiba, Japan.

Corresponding authors: Shinji Kume, M.D., Ph.D., and Shin-ichi Araki, M.D., Ph.D.
Department of Medicine, Shiga University of Medical Science,
Tsukinowa-cho, Seta, Otsu, Shiga 520-2192, Japan.
Tel: +81-775-48-2222; Fax: +81-775-48-3858; E-mail: skume@belle.shiga-med.ac.jp (S.K.) and araki@belle.shiga-med.ac.jp (A.S-i.)

Abstract

To examine the cell-protective role of podocyte autophagy against glomerular endothelial dysfunction in diabetes, we analyzed the renal phenotype of tamoxifen (TM)-inducible podocyte-specific Atg5-deficient (iPodo-Atg5$^{-/-}$) mice with experimental endothelial dysfunction. In both control and iPodo-Atg5$^{-/-}$ mice, high fat diet (HFD) feeding induced glomerular endothelial damage characterized by decreased urinary nitric oxide (NO) excretion, collapsed endothelial fenestrae, and reduced endothelial glycocalyx. HFD-fed control mice showed slight albuminuria and nearly normal podocyte morphology. In contrast, HFD-fed iPodo-Atg5$^{-/-}$ mice developed massive albuminuria accompanied by severe podocyte injury that was observed predominantly in podocytes adjacent to damaged endothelial cells by scanning electron microscopy. Although podocyte-specific autophagy deficiency did not affect endothelial NO synthase deficiency-associated albuminuria, it markedly exacerbated albuminuria and severe podocyte morphological damage when the damage was induced by intravenous neuraminidase injection to remove glycocalyx from the endothelial surface. Furthermore, endoplasmic reticulum stress was accelerated in podocytes of iPodo-Atg5$^{-/-}$ mice stimulated with neuraminidase, and treatment with molecular chaperone tauroursodeoxycholic acid improved neuraminidase-induced severe albuminuria and podocyte injury. In conclusion, podocyte autophagy plays a renoprotective role against diabetes-related structural endothelial damage, providing an additional insight into the pathogenesis of massive proteinuria in diabetic nephropathy.

Key words: Podocytes, massive proteinuria, diabetic kidney disease, autophagy, mitochondria

Introduction

Massive proteinuria is a strong risk for renal dysfunction in diabetic kidney disease (DKD) [1,2]. Thus, revealing the mechanism underlying this condition is urgently required. The glomerular filtration barrier consists of an endothelium, glomerular basement membrane, and podocytes. Among these components, podocyte damage is strongly associated with massive proteinuria in DKD [3,4]. However, considering that DKD is initially characterized by a microvascular complication, in which endothelial damage is considered as the first event [5,6], there must be a mechanism of progression from endothelial to podocyte damage.

Glomerular endothelial cells have a unique structural feature characterized by fenestration to filter waste products and glycocalyx with a negative charge to prevent albumin leakage into urine [7-9]. Furthermore, endothelial cells functionally secrete nitric oxide (NO) in nitric oxide synthase 3 (NOS3)-dependent manner to maintain a normal glomerular environment [10]. Metabolic alterations in diabetes impair endothelial cells, leading to microalbuminuria. Furthermore, the endothelial damage has been reported to be involved in the development of podocyte damage [11,12]. However, the pathological process from endothelial damage to podocyte damage in diabetes has not been fully understood.

Autophagy is an intracellular degradation system that overcomes various stress conditions in many cell types [13]. Autophagic activity in podocytes is considerably higher than in other mammalian cell type [14], suggesting that this system is essential for podocyte functions. Some reports demonstrated that podocyte autophagy plays cell-

protective roles in diabetes [15], however its role in podocyte protection against glomerular endothelial cell damage in diabetes has not been elucidated.

In this study, we hypothesized that autophagy is required to protect podocytes from cytotoxic stress related to endothelial damage in diabetes, and that impaired podocyte autophagy is involved in the progression from endothelial to podocyte damage in DKD. To test these hypotheses, we analyzed the renal phenotypes of a newly established inducible podocyte-specific autophagy-deficient mouse model under diabetes-related structural and functional endothelial damage.

Results

Characterization of functional and structural endothelial damage in high-fat diet (HFD)-induced diabetic mice

HFD treatment increased body weight gain and fasting blood glucose levels during 32 weeks of dietary intervention compared with mice fed the standard diet (STD) (Fig. 1A and B). In HFD-fed mice, urinary NO excretion was significantly decreased from 4 weeks after the dietary intervention compared with STD-fed mice (Fig. 1C). Changes in endothelial cell morphology were characterized by the disappearance of endothelial fenestrae and increasing microblebs in scanning electron microscopy (EM) analysis and decreased glycocalyx determined by isolectin and wheat germ agglutinin (WGA) staining started from 8 weeks after HFD feeding (Fig. 1D). These results suggested that the HFD intervention caused both functional and structural endothelial damage in glomeruli of mice.

Generation of tamoxifen (TM)-inducible podocyte-specific Atg5-deficient (iPodo-Atg5$^{-/-}$) mice

Eight-week-old male Atg5$^{f/f}$ mice and Atg5$^{f/f}$ mice carrying podocyte-specific CreERT2 were fed either the STD or HFD (Supplemental Fig. 1A). Then, TM was injected into the mice at 8 weeks after the dietary intervention to delete the *Atg5* gene in podocytes.

At 8 weeks after the TM injection, the HFD-induced body weight gain and increase in fasting blood glucose levels were not different between both genotypes (Supplemental Fig. 1B and C). SQSTM1 protein accumulation is an indicator of cellular

autophagy insufficiency [16]. SQSTM1 was accumulated in the podocytes of STD-fed iPodo-Atg5$^{-/-}$ mice, which was increased by HFD feeding (Fig. 2A). These data indicated that the HFD-induced obese diabetic condition increased the need for autophagy in podocytes.

Severe podocyte injury in HFD-fed iPodo-Atg5$^{-/-}$ mice

HFD intervention increased urinary albumin excretion in control mice, which was exacerbated in HFD-fed iPodo-Atg5$^{-/-}$ mice at 4 and 8 weeks after the TM injection (Fig. 2B and C). Although glomerular sclerotic lesions induced by HFD feeding were similar between two genotypes, podocyte foot process effacement in scanning EM and decreased podocin expression were more severe in HFD-fed iPodo-Atg5$^{-/-}$ mice (Fig. 2A). In addition, podocin staining became pathogenically granular pattern in HFD-fed iPodo-Atg5$^{-/-}$, and the podocyte number determined by counting WT-1-positive cells was significantly decreased in HFD-fed iPodo-Atg5$^{-/-}$ mice (Fig. 2A and D).

Pathological interaction between endothelial damage and deficient podocyte autophagy in podocyte damage of HFD-fed iPodo-Atg5$^{-/-}$ mice

Next, we evaluated the spatial interaction between damaged endothelial cells and damaged podocytes by scanning EM (Fig. 3A). HFD-fed Atg5$^{f/f}$ mice showed a normal podocyte architecture despite being adjacent to damaged endothelial cells (Fig. 3A). In HFD-fed iPodo-Atg5$^{-/-}$ mice, podocyte injury was observed particularly in the podocytes adjacent to damaged endothelial cells. However, if an endothelial cell was undamaged,

the adjacent podocytes retained their normal morphology (Fig. 3A). To confirm this pathological interaction, we conducted isolectin and desmin double staining (Supplemental Fig. 2A-D). Desmin expression is a marker of podocyte damage. In HFD-fed $Atg5^{f/f}$ mice, desmin staining was less observed regardless of positive or negative staining by isolectin (Supplemental Fig. 2A and B), whereas in HFD-fed iPodo-$Atg5^{-/-}$ mice, desmin staining was markedly observed particularly nearby podocytes, where isolectin staining was absent (Supplemental Fig. 2C and D). These results suggested that endothelial cell damage was a trigger of podocyte damage in HFD-fed iPodo-$Atg5^{-/-}$ mice.

No involvement of NO deficiency in severe injury of autophagy-deficient podocytes

Because HFD-fed mice showed functional and structural endothelial damage, we next elucidated which played the main pathological role in severe podocyte injury of diabetic mice with deficient podocyte autophagy. To this end, we first generated iPodo-$Atg5^{-/-}$ mice lacking NOS3 systemically (Supplemental Fig. 3A). $NOS3^{-/-}$ mice showed mild albuminuria at 4 and 8 weeks after the TM injection, but this albuminuria was not enhanced by the autophagy deficiency in podocytes (Supplemental Fig. 3B and C). Furthermore, morphological changes of podocyte foot processes, podocin expression levels (Supplemental Fig. 3D), suggesting that functional endothelial damage was not a trigger of podocyte injury in HFD-fed iPodo-$Atg5^{-/-}$ mice.

Pathological role of glycocalyx disappearance in severe injury of autophagy-deficient podocytes

We next examined a possibility that structural endothelial damage might be involved in severe podocyte injury of HFD-fed iPodo-Atg5$^{-/-}$ mice. To examine this possibility, we used neuraminidase that transiently removes endothelial glycocalyx. In fact, an intravenous injection of neuraminidase decreased the density of WGA staining at day 1 after the injection, which was recovered at day 3 after the injection, although nephrin expression was not altered (Supplemental Fig. 4A). Neuraminidase was then injected into in STD-fed Atg5$^{f/f}$ mice and STD-fed iPodo-Atg5$^{-/-}$ mice (Supplemental Fig. 4B). The neuraminidase treatment led to mild transient albuminuria in STD-fed Atg5$^{f/f}$ mice (Fig. 3B). Podocyte autophagy deficiency significantly magnified the albuminuria at days 1 and 2 after the injection (Fig.3B), which was accompanied by alterations of the foot process structure and podocin expression pattern (Fig. 3C and supplemental Fig.4C). These results suggested that podocyte autophagy has a podocyte protective role against structural endothelial cell damage.

Pathological role of albumin in cell damage in autophagy-deficient podocytes.

Because removal of glycocalyx should increase albumin leaking into Bowman's space, leading to high exposure of albumin to podocytes, we hypothesized that increased albumin exposure caused cell damage in autophagy-deficient podocytes. To explore this hypothesis, we used cultured autophagy-deficient podocytes. The protein coded by the *Atg7* gene is essential for autophagosome formation [15,17]. We stimulated the cultured Atg7-deficient podocytes and control Atg7$^{f/f}$ podocytes with albumin. Albumin treatment increased apoptosis determined by cleavage of caspase 3, which was enhanced by

autophagy deficiency (Fig. 4A and B).

Involvement of enhanced endoplasmic reticulum (ER) stress in severe podocyte injury of autophagy-deficient podocytes exposed to albumin

To determine which intracellular pathway or whether organelle damage was associated with the enhanced apoptosis in autophagy-deficient podocytes stimulated by albumin, proteomic analysis followed by pathway analysis related to apoptosis events was applied. The analysis suggested that enhanced ER stress was strongly involved in the autophagy-deficiency-related acceleration of apoptosis in podocytes (Fig. 4C). In fact, in the podocytes of STD-fed iPodo-Atg5$^{-/-}$ mice treated with neuraminidase, C/EBP homologous protein (CHOP), an inducer of ER stress-related apoptosis [18,19], was increased significantly (Fig. 4D). Finally, the mice were treated with tauroursodeoxycholic acid (TUDCA), a molecular chaperone, to enhance ER capacity and subsequently reduce ER stress [20]. TUDCA treatment significantly decreased urinary albumin excretion (Fig. 4E). Furthermore, the altered foot process structure and podocin expression pattern were ameliorated by TUDCA treatment in STD-fed iPodo-Atg5$^{-/-}$ mice treated with neuraminidase (Fig. 4F).

Discussion

The present study provides the evidence that podocyte autophagy is of particular importance to protect cells against endothelial damage-related cytotoxicity in diabetes.

One of main points in this study is that we used a drug-inducible podocyte-specific autophagy-deficient mouse model. Previous studies, including ours, have used a congenital genetically modified mouse model [14,15]. It has been a concern that enhancement of a decomposition system other than autophagy may occur in a compensating manner in podocytes of this mouse model. In fact, in our previous study, congenital podocyte-specific autophagy-deficient mice showed severe podocyte injury after 32 weeks of HFD intervention [15], whereas the inducible autophagy-deficient mice developed severe damage after only 8 weeks of HFD intervention. These results support such a concern and provide evidence that autophagy *per se* is an important cell-protective mechanism during disease states including diabetes.

As shown in this study, two types of endothelial abnormality are characterized during the development of HFD-induced obese diabetes. One is a structural alteration with decreased glycocalyx, and the other is functional damage by NO deficiency. The NO deficiency is strongly associated with progression of podocyte damage in diabetes [11], which is partly associated with mitochondrial damage. Damaged mitochondria can be removed by autophagy machinery [21]. Therefore, we initially hypothesized that podocyte-specific autophagy deficiency may exacerbate podocyte injury due to the NO deficiency by enhancing mitochondrial damage. However, this was not observed. In contrast, the autophagy deficiency worsened podocyte injury mediated by neuraminidase-

mediated removal of glycocalyx, the structural barrier in glomeruli, suggesting that podocyte autophagy removes a cytotoxic molecule that passes through the damaged endothelium. Based on our results, serum albumin may be a candidate molecule that causes podocyte injury during endothelial damage, and autophagy protects podocytes from albumin-induced cytotoxicity.

A high level of basal autophagy in podocytes has been reported [14], although its exact role remains unclear. Based on our results, podocytes may maintain basal autophagy at a high level to rapidly respond to cellular toxicity caused by abrupt endothelial damage. If this is the case, in the situation of diabetes leading to endothelial damages, it is not surprising that autophagy insufficiency leads to severe podocyte damage. In clinical settings, even if patients show hyperglycemia to the same extent, the incidence and progression of proteinuria vary from person to person. The difference in the vulnerability of cytoprotective mechanisms including podocyte autophagy in an individual may be responsible for the variety of renal manifestations in diseases associated with endothelial damage. To protect terminally differentiated podocytes that do not have a replicative capacity, mammals may have developed dual protective systems, an endothelial glycocalyx-related structural barrier and intracellular adaptive mechanism in podocytes against certain serum factors that pass through the damaged endothelium, and diabetes may disturb both.

Autophagy targets various organelles under stress conditions, such as mitochondria, ER, peroxisomes, and lysosomes [22,23]. Among these, ER appears to be a target to be protected by autophagy in podocytes during structural endothelial damage.

ER stress has been reported to be involved in the pathogenesis of podocyte damage in DKD [24,25], but the mechanism underlying enhanced diabetes-related ER stress has not been fully elucidated. Autophagy insufficiency may be involved in the diabetes-related enhancement of ER stress, and amelioration of the altered autophagy-ER axis in diabetes may be an effective to prevent the progression of DKD with massive proteinuria.

Some issues remain in this study. First, which serum factors pass through the damaged endothelium and cause podocyte damage have not been clearly identified. Based on our study, albumin is a candidate molecule, but there may be other factors involved in the pathology. In particular, increased levels of fatty acid-bound albumin and advanced glycated end-products in diabetes may be more toxic than pure albumin [5,26]. Identifying the serum factor(s) may facilitate development of a novel therapeutic strategy for DKD. Second, a reason why deficient autophagy did not exacerbate albuminuria in $NOS3^{-/-}$ mice remains unclear. Our cell culture study clearly showed that albumin stimulation worsened apoptosis in the autophagy-deficient podocytes, but podocyte autophagy deficiency in mice did not show severe albuminuria in $NOS3^{-/-}$ mice although they showed mild albuminuria. Considering that $NOS3^{-/-}$-iPodo-$Atg5^{-/-}$ kept almost normal endothelial structure, there might be some difference in significance or cause between NOS3 deficiency-dependent albuminuria and structural damage-dependent albuminuria. Further examination is required to conclude this concern.

In conclusion, autophagy protects podocytes from diabetes-related structural endothelial damage. Insufficient autophagy leads to severe podocyte injury and subsequent massive albuminuria by activation of ER stress during the development of

endothelial damage in DKD. The present findings suggest a novel role of podocyte autophagy in the pathogenesis of DKD and shed new light on the development of therapies for the disease.

Methods

Ethics and Animal studies

All animal handling and experimentation were conducted according to the guidelines of the Research Center for Animal Life Science at Shiga University of Medical Science. All experimental protocols were approved by the Gene Recombination Experiment Safety Committee and the Research Center for Animal Life Science at Shiga University of Medical Science. Detailed animal study protocols used in this study is described in Supplemental Method.

Histological analyses

Periodic acid-Schiff (PAS) staining, immunofluorescence, and immunohistochemistry analyses were performed as described previously [27]. Antibodies against SQSTM1 (MBL, Tokyo, Japan), WT1 (Santa Cruz Biotechnology, Santa Cruz, CA), podocin (Sigma-Aldrich), nephrin (PROGEN, Heidelberg, Germany), desmin, and CHOP (Cell Signaling, Danvers, MA) were used. Corresponding fluorescently labeled secondary antibodies (goat anti-mouse IgG-Alexa, goat anti-rabbit IgG-Alexa, and goat anti-rat IgG-Alexa Sigma-Aldrich) were used. Two kinds of lectins, isolectin (Isolectin GS-IB4 from *griffonia simplicifolia*) and WGA from Thermo Fisher (Waltham, MA) were used to evaluate glycocalyx. EM analyses were performed with an S-570 and H-7500 (Hitachi, Tokyo, Japan). To determine the podocyte number, WT1-positive cells were counted in more than 10 glomeruli in each mouse sample. To determine ER stress in podocytes, CHOP-positive cells in glomeruli were counted in more than 10 glomeruli in each mouse

sample.

Blood and urinary analyses

Blood glucose levels were measured using a Glutest sensor (SanwaKagaku, Nagoya, Japan). Urinary albumin excretions were measured by a turbidimetric immunoassay and urinary creatine levels were measured by an enzytec generic (ORIENNTAL YEASR Co., LTD, Tokyo, Japan). Urinary albumin excretion levels are expressed as $\log_{10}$ ratio urinary albumin/creatinine. Urinary NO excretion levels were measured by a fluorometric nitric oxide assay kit (abcam, Cambridge, UK).

Western blot analysis

An Atg7-deficient podocyte cell line was established with the pMESVTS plasmid containing a SV40 large T antigen [28]. Glomeruli of podocyte-specific Atg7-deficient [17,29] and wildtype mice were isolated using Dynabeads M-450 Tosylactivated (Invitrogen, Carlsbad, CA) [30]. Podocytes were infected with a viral supernatant from PLAT-E cells transfected with the pMESVTS plasmid [31] and maintained in RPMI-1640 with 10% FBS at 33°C. The cells were cultured at 39°C to induce differentiation over 7 days. Proten samples were collected from differentiated Atg-7-deficient and wildtype podocytes stimulated with 5 g/dl bovine serum albumin for 30 hours. Western blot analysis was performed as described previously [32]. The membranes were incubated with antibodies against cleaved caspase 3 (Asp175) (Cell Signaling Technology, Danvers, MA), Atg7 (Cell Signaling Technology, Danvers, MA), or β-actin (Sigma-Aldrich).

Proteomic analyses

The proteomic analysis was conducted by Medical Proteoscope (Kanagawa, Japan). Whole data are included as Supplemental Data. Proteomic analysis was performed as previously reported [33]. Method for Bioinformatic analysis is described in Supplemental Method.

Statistical Analyses

Results are expressed as the mean ± SEM. Analysis of variance and Tukey's post-hoc test were used to determine significant differences for multiple comparisons. The Student's t-test was used for comparisons between two groups. $P < 0.05$ was considered as statistically significant.

Acknowledgments

We thank Naoko Yamanaka (Shiga University of Medical Science), and the Central Research Laboratory of Shiga University of Medical Science for technical assistance.

Funding

This study was supported by Grants-in-Aid for Scientific Research (KAKENHI) from the Japan Society for the Promotion of Science (25713033 to S.K. and 26293217 to H.M.), grants from the Japan Diabetes Foundation (to S.K.) and Takeda Medical Foundation (to S.K.), an MSD Grant (to S.K.), and the Lilly Grant Office (to S.K.) and Bayer Academic Support (to H.M.) and Otsuka Pharmaceutical (to S-i. A.) and Torii Pharmaceutical (to S-i. A.).

Competing interests

The authors declare no competing interests.

References

[1] A.S. Krolewski, Progressive renal decline: the new paradigm of diabetic nephropathy in type 1 diabetes, Diabetes Care 38 (2015) 954-962. 10.2337/dc15-0184.

[2] A.S. Krolewski, J. Skupien, P. Rossing, J.H. Warram, Fast renal decline to end-stage renal disease: an unrecognized feature of nephropathy in diabetes, Kidney Int 91 (2017) 1300-1311. 10.1016/j.kint.2016.10.046.

[3] K.E. White, R.W. Bilous, S.M. Marshall, M. El Nahas, G. Remuzzi, G. Piras, S. De Cosmo, G. Viberti, Podocyte number in normotensive type 1 diabetic patients with albuminuria, Diabetes 51 (2002) 3083-3089. 10.2337/diabetes.51.10.3083.

[4] M.E. Pagtalunan, P.L. Miller, S. Jumping-Eagle, R.G. Nelson, B.D. Myers, H.G. Rennke, N.S. Coplon, L. Sun, T.W. Meyer, Podocyte loss and progressive glomerular injury in type II diabetes, J Clin Invest 99 (1997) 342-348. 10.1172/JCI119163.

[5] M. Brownlee, Biochemistry and molecular cell biology of diabetic complications, Nature 414 (2001) 813-820. 10.1038/414813a.

[6] M. Brownlee, The pathobiology of diabetic complications: a unifying mechanism, Diabetes 54 (2005) 1615-1625. 10.2337/diabetes.54.6.1615.

[7] N. Jourde-Chiche, F. Fakhouri, L. Dou, J. Bellien, S. Burtey, M. Frimat, P.A. Jarrot, G. Kaplanski, M. Le Quintrec, V. Pernin, C. Rigothier, M. Sallée, V. Fremeaux-Bacchi, D. Guerrot, L.T. Roumenina, Endothelium structure and function in kidney health and disease, Nat Rev Nephrol 15 (2019) 87-108. 10.1038/s41581-018-0098-z.

[8] T.J. Rabelink, D. de Zeeuw, The glycocalyx--linking albuminuria with renal and cardiovascular disease, Nat Rev Nephrol 11 (2015) 667-676. 10.1038/nrneph.2015.162.

[9] B.M. van den Berg, G. Wang, M.G.S. Boels, M.C. Avramut, E. Jansen, W.M.P.J. Sol, F. Lebrin, A. Jan van Zonneveld, E.J.P. de Koning, H. Vink, H.J. Gröne, P. Carmeliet, J. van der Vlag, T.J. Rabelink, Glomerular Function and Structural Integrity Depend on Hyaluronan Synthesis by Glomerular Endothelium, J Am Soc Nephrol (2019). 10.1681/ASN.2019020192.

[10] T. Takahashi, R.C. Harris, Role of endothelial nitric oxide synthase in diabetic nephropathy: lessons from diabetic eNOS knockout mice, J Diabetes Res 2014 (2014) 590541. 10.1155/2014/590541.

[11] S. Ueda, S. Ozawa, K. Mori, K. Asanuma, M. Yanagita, S. Uchida, T. Nakagawa, ENOS deficiency causes podocyte injury with mitochondrial abnormality, Free Radic Biol Med 87 (2015) 181-192. 10.1016/j.freeradbiomed.2015.06.028.

[12] F.S. Siddiqi, A. Advani, Endothelial-podocyte crosstalk: the missing link between endothelial dysfunction and albuminuria in diabetes, Diabetes 62 (2013) 3647-3655. 10.2337/db13-0795.

[13] N. Mizushima, A. Yamamoto, M. Matsui, T. Yoshimori, Y. Ohsumi, In vivo analysis of autophagy in response to nutrient starvation using transgenic mice expressing a fluorescent autophagosome marker, Mol Biol Cell 15 (2004) 1101-1111. 10.1091/mbc.e03-09-0704.

[14] B. Hartleben, M. Gödel, C. Meyer-Schwesinger, S. Liu, T. Ulrich, S. Köbler, T. Wiech, F. Grahammer, S.J. Arnold, M.T. Lindenmeyer, C.D. Cohen, H. Pavenstädt, D. Kerjaschki, N. Mizushima, A.S. Shaw, G. Walz, T.B. Huber, Autophagy influences glomerular disease susceptibility and maintains podocyte homeostasis in aging mice, J Clin Invest 120 (2010) 1084-1096. 10.1172/JCI39492.

[15] A. Tagawa, M. Yasuda, S. Kume, K. Yamahara, J. Nakazawa, M. Chin-Kanasaki, H. Araki, S. Araki, D. Koya, K. Asanuma, E.H. Kim, M. Haneda, N. Kajiwara, K. Hayashi, H. Ohashi, S. Ugi, H. Maegawa, T. Uzu, Impaired Podocyte Autophagy Exacerbates Proteinuria in Diabetic Nephropathy, Diabetes 65 (2016) 755-767. 10.2337/db15-0473.

[16] S. Pankiv, T.H. Clausen, T. Lamark, A. Brech, J.A. Bruun, H. Outzen, A. Øvervatn, G. Bjørkøy, T. Johansen, p62/SQSTM1 binds directly to Atg8/LC3 to facilitate degradation of ubiquitinated protein aggregates by autophagy, J Biol Chem 282 (2007) 24131-24145. 10.1074/jbc.M702824200.

[17] M. Komatsu, S. Waguri, T. Ueno, J. Iwata, S. Murata, I. Tanida, J. Ezaki, N. Mizushima, Y. Ohsumi, Y. Uchiyama, E. Kominami, K. Tanaka, T. Chiba, Impairment of starvation-induced and constitutive autophagy in Atg7-deficient mice, J Cell Biol 169 (2005) 425-434. 10.1083/jcb.200412022.

[18] S.J. Marciniak, C.Y. Yun, S. Oyadomari, I. Novoa, Y. Zhang, R. Jungreis, K. Nagata, H.P. Harding, D. Ron, CHOP induces death by promoting protein synthesis and oxidation in the stressed endoplasmic reticulum, Genes Dev 18 (2004) 3066-3077. 10.1101/gad.1250704.

[19] H. Zinszner, M. Kuroda, X. Wang, N. Batchvarova, R.T. Lightfoot, H. Remotti, J.L. Stevens, D. Ron, CHOP is implicated in programmed cell death in response to impaired function of the endoplasmic reticulum, Genes Dev 12 (1998) 982-995. 10.1101/gad.12.7.982.

[20] U. Ozcan, E. Yilmaz, L. Ozcan, M. Furuhashi, E. Vaillancourt, R.O. Smith, C.Z.

Görgün, G.S. Hotamisligil, Chemical chaperones reduce ER stress and restore glucose homeostasis in a mouse model of type 2 diabetes, Science 313 (2006) 1137-1140. 10.1126/science.1128294.
[21] G. Ashrafi, T.L. Schwarz, The pathways of mitophagy for quality control and clearance of mitochondria, Cell Death Differ 20 (2013) 31-42. 10.1038/cdd.2012.81.
[22] G. Kroemer, G. Mariño, B. Levine, Autophagy and the integrated stress response, Mol Cell 40 (2010) 280-293. 10.1016/j.molcel.2010.09.023.
[23] N. Mizushima, M. Komatsu, Autophagy: renovation of cells and tissues, Cell 147 (2011) 728-741. 10.1016/j.cell.2011.10.026.
[24] K. Inoki, H. Mori, J. Wang, T. Suzuki, S. Hong, S. Yoshida, S.M. Blattner, T. Ikenoue, M.A. Rüegg, M.N. Hall, D.J. Kwiatkowski, M.P. Rastaldi, T.B. Huber, M. Kretzler, L.B. Holzman, R.C. Wiggins, K.L. Guan, mTORC1 activation in podocytes is a critical step in the development of diabetic nephropathy in mice, J Clin Invest 121 (2011) 2181-2196. 10.1172/JCI44771.
[25] T. Madhusudhan, H. Wang, W. Dong, S. Ghosh, F. Bock, V.R. Thangapandi, S. Ranjan, J. Wolter, S. Kohli, K. Shahzad, F. Heidel, M. Krueger, V. Schwenger, M.J. Moeller, T. Kalinski, J. Reiser, T. Chavakis, B. Isermann, Defective podocyte insulin signalling through p85-XBP1 promotes ATF6-dependent maladaptive ER-stress response in diabetic nephropathy, Nat Commun 6 (2015) 6496. 10.1038/ncomms7496.
[26] Y. Tanaka, S. Kume, M. Chin-Kanasaki, H. Araki, S.I. Araki, S. Ugi, T. Sugaya, T. Uzu, H. Maegawa, Renoprotective effect of DPP-4 inhibitors against free fatty acid-bound albumin-induced renal proximal tubular cell injury, Biochem Biophys Res Commun 470 (2016) 539-545. 10.1016/j.bbrc.2016.01.109.
[27] S. Kume, T. Uzu, S. Araki, T. Sugimoto, K. Isshiki, M. Chin-Kanasaki, M. Sakaguchi, N. Kubota, Y. Terauchi, T. Kadowaki, M. Haneda, A. Kashiwagi, D. Koya, Role of altered renal lipid metabolism in the development of renal injury induced by a high-fat diet, J Am Soc Nephrol 18 (2007) 2715-2723. 10.1681/ASN.2007010089.
[28] G.H. Lee, K. Ogawa, N.R. Drinkwater, Conditional transformation of mouse liver epithelial cells. An in vitro model for analysis of genetic events in hepatocarcinogenesis, Am J Pathol 147 (1995) 1811-1822.
[29] J.A. Oliva Trejo, K. Asanuma, E.H. Kim, M. Takagi-Akiba, K. Nonaka, T. Hidaka, M. Komatsu, N. Tada, T. Ueno, Y. Tomino, Transient increase in proteinuria, poly-ubiquitylated proteins and ER stress markers in podocyte-specific autophagy-deficient

mice following unilateral nephrectomy, Biochem Biophys Res Commun 446 (2014) 1190-1196. 10.1016/j.bbrc.2014.03.088.
[30] M. Takemoto, N. Asker, H. Gerhardt, A. Lundkvist, B.R. Johansson, Y. Saito, C. Betsholtz, A new method for large scale isolation of kidney glomeruli from mice, Am J Pathol 161 (2002) 799-805. 10.1016/S0002-9440(10)64239-3.
[31] S. Morita, T. Kojima, T. Kitamura, Plat-E: an efficient and stable system for transient packaging of retroviruses, Gene Ther 7 (2000) 1063-1066. 10.1038/sj.gt.3301206.
[32] Y. Tanaka, S. Kume, S. Araki, K. Isshiki, M. Chin-Kanasaki, M. Sakaguchi, T. Sugimoto, D. Koya, M. Haneda, A. Kashiwagi, H. Maegawa, T. Uzu, Fenofibrate, a PPARα agonist, has renoprotective effects in mice by enhancing renal lipolysis, Kidney Int 79 (2011) 871-882. 10.1038/ki.2010.530.
[33] S. Sugahara, S. Kume, M. Chin-Kanasaki, I. Tomita, M. Yasuda-Yamahara, K. Yamahara, N. Takeda, N. Osawa, M. Yanagita, S.I. Araki, H. Maegawa, Protein O-GlcNAcylation Is Essential for the Maintenance of Renal Energy Homeostasis and Function, J Am Soc Nephrol 30 (2019) 962-978. 10.1681/ASN.2018090950.

Figure legends

Figure 1. High-fat diet (HFD)-induced functional and structural glomerular endothelial cell damage. (A and B) Changes in body weight (A) and fasting blood glucose levels (B) in mice fed either standard diet (STD) or HFD during the 32-week experimental period. (C) Urinary nitric oxide (NO) levels in the two groups of mice. (D) Time-dependent structural changes in glomerular endothelial cells of HFD-fed mice. Scanning electron microscopy (EM) and immunofluorescence (IF) for isolectin and Wheat Germ Agglutinin (WGA). Original magnification, ×20,000 for scanning EM, ×1,000 for IF. All results are presented as mean ± SEM. *P < 0.05, **P < 0.01. NS: not significant.

Figure 2. Severe podocyte injury in high-fat diet (HFD)-fed iPodo-Atg5$^{-/-}$ mice. (A) Representative pictures of immunohistochemistry (IHC) for SQSTM1, a marker of autophagy insufficiency, PAS staining, scanning electron microscopy (EM), immunofluorescence (IF) of podocin and IHC for WT1 in four groups of mice. Original magnification, ×400 for SQSTM1, PAS staining and WT-1, ×8,000 for scanning EM, ×1,000 for IF of podocin. (B, C) Urinary albumin excretion levels in the indicated mouse groups at 4 weeks (B) and 8 weeks (C) after the tamoxifen injection. Urinary albumin excretion levels are expressed as $\log_{10}$ ratio urinary albumin/creatinine. (D) Quantitation of WT1-positive podocytes in glomeruli. All results are presented as mean ± SEM. *P < 0.05, **P < 0.01. NS: not significant.

Figure 3. Severe podocyte injury in iPodo-Atg5$^{-/-}$ mice with neuraminidase-induced structural endothelial dysfunction. (A) Scanning electron microscopy (EM) of glomeruli from HFD-fed Atg5$^{f/f}$ and HFD-fed iPodo-Atg5$^{-/-}$ mice. Original magnification: ×8,000 and ×20,000 for details. (B) Time-dependent changes in urinary albumin excretion level in neuraminidase-injected Atg5$^{f/f}$ and iPodo-Atg5$^{-/-}$ mice. (C) Scanning electron microscopy (EM) of podocytes. Original magnification: ×8,000. All results are presented as mean ± SEM. *P < 0.05, **P < 0.01. NS: not significant.

Figure 4. Enhanced endoplasmic reticulum (ER) stress iPodo-Atg5$^{-/-}$ mice with structural endothelial dysfunction. (A) Western blots of Atg7, cleaved caspase 3, and

β-actin in cultured $Atg7^{f/f}$ and $Atg7^{-/-}$ podocytes stimulated with/without 5 g/dl bovine serum albumin. (B) Quantitative ratios of cleaved caspase 3 to β-actin (n=4). (C) Pathological event analysis of data from the proteomic analysis. The details of each calculated score, (p), (v), and (c), are explained in the Supplemental Method. (D) Immunohistochemical (IHC) for C/EBP homologous protein (CHOP). Original magnification: ×400. Semiquantitative measurement of CHOP-positive cells in glomeruli. (E) Urinary albumin excretion level in vehicle and TUDCA-treated groups. (D) Scanning electron microscopy (EM), immunofluorescent (IF) for podocin. Original magnification, ×8,000 for scanning EM, and ×1,000 for IF of podocin and. All results are presented as mean ± SEM. *P < 0.05. NS: not significant.

Figure 1

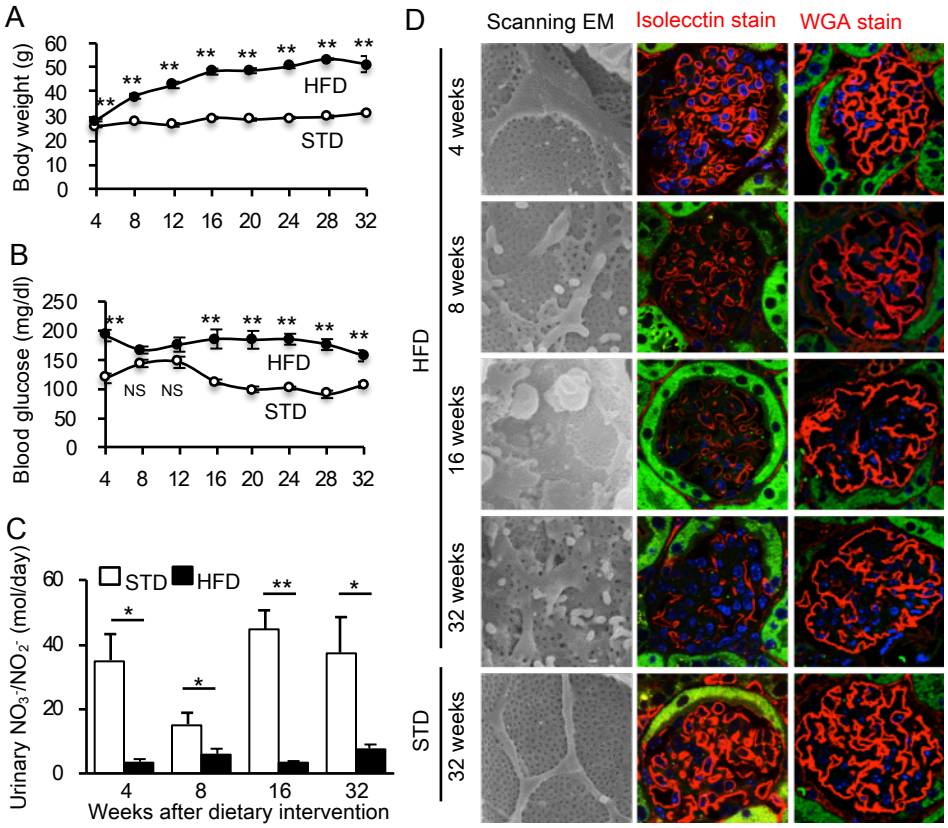
A
Body weight (g)
HFD
STD
B
Blood glucose (mg/dl)
HFD
STD
NS
C
Urinary NO3-/NO2- (mol/day)
STD
HFD
Weeks after dietary intervention
D
Scanning EM
Isolecctin stain
WGA stain
HFD
STD
4 weeks
8 weeks
16 weeks
32 weeks
32 weeks

Figure 2

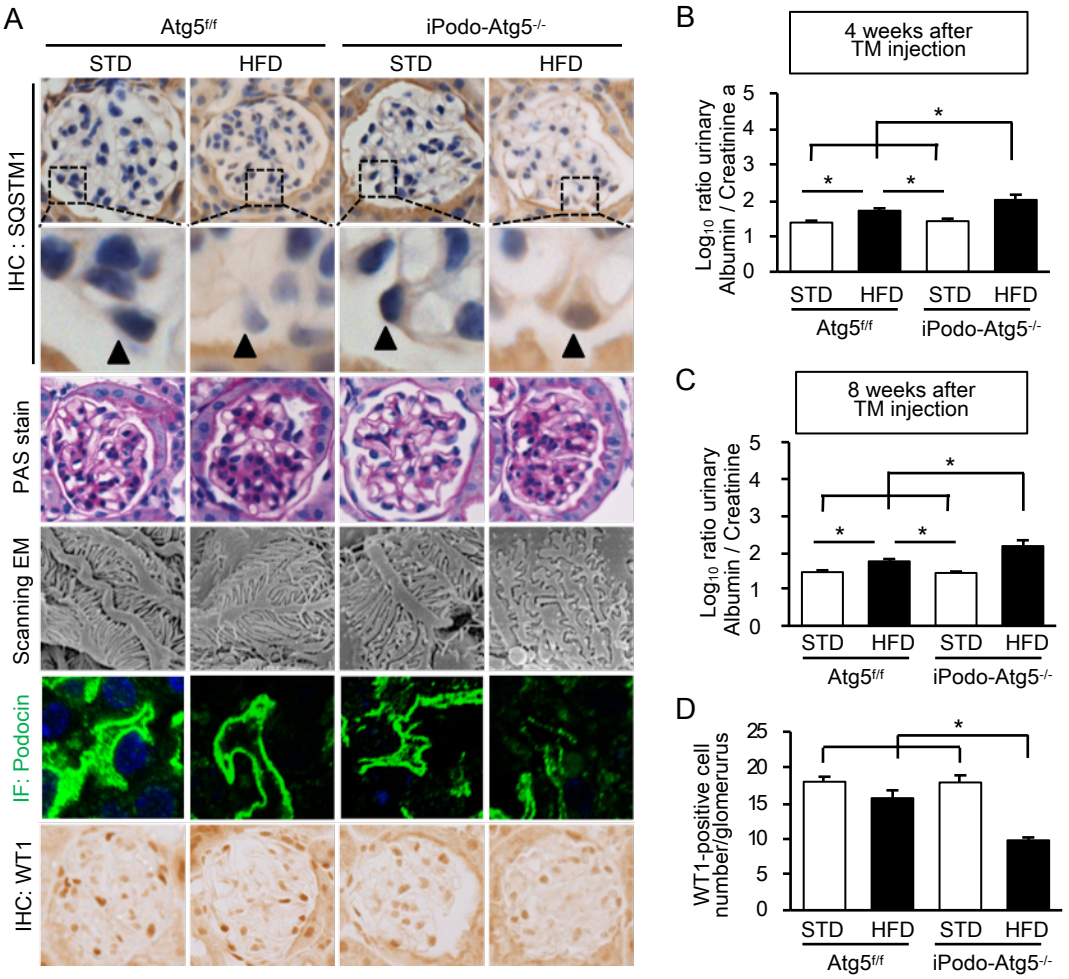
A
Atg5f/f
iPodo-Atg5-/-
STD
HFD
STD
HFD
IHC : SQSTM1
PAS stain
Scanning EM
IF: Podocin
IHC: WT1
B
4 weeks after TM injection
Log10 ratio urinary Albumin / Creatinine a
STD
HFD
STD
HFD
Atg5f/f
iPodo-Atg5-/-
C
8 weeks after TM injection
Log10 ratio urinary Albumin / Creatinine
STD
HFD
STD
HFD
Atg5f/f
iPodo-Atg5-/-
D
WT1-positive cell number/glomerurus
STD
HFD
STD
HFD
Atg5f/f
iPodo-Atg5-/-

Figure 3

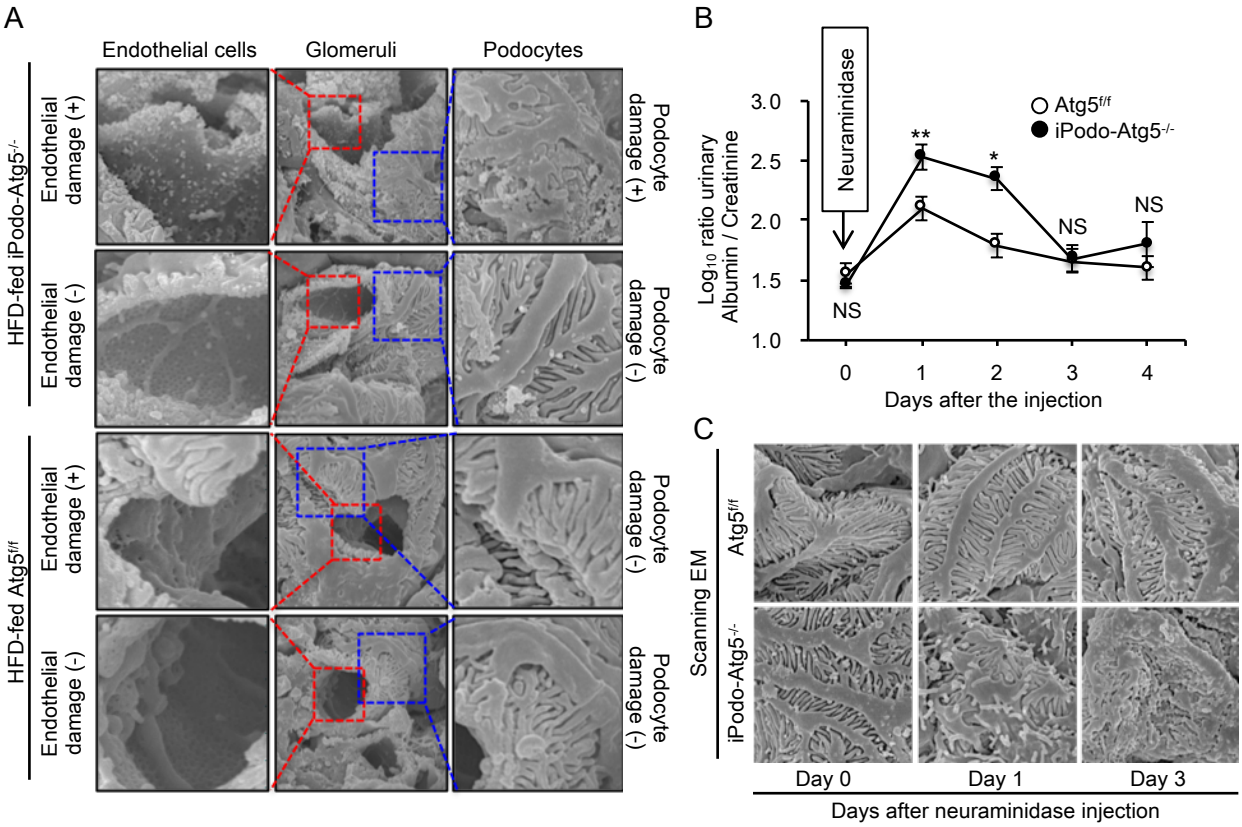
A
Endothelial cells
Glomeruli
Podocytes
HFD-fed iPodo-Atg5-/-
Endothelial damage (+)
Endothelial damage (-)
HFD-fed Atg5f/f
Podocyte damage (+)
Podocyte damage (-)
B
Neuraminidase
Atg5f/f
iPodo-Atg5-/-
Log10 ratio urinary Albumin / Creatinine
3.0
2.5
2.0
1.5
1.0
**
*
NS
NS
NS
0
1
2
3
4
Days after the injection
C
Scanning EM
Atg5f/f
iPodo-Atg5-/-
Day 0
Day 1
Day 3
Days after neuraminidase injection

Figure 4

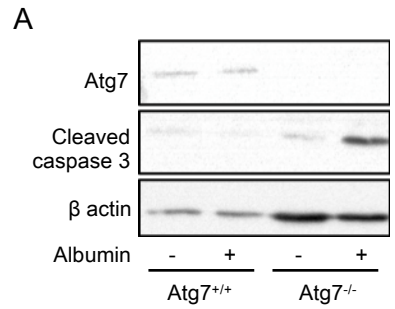

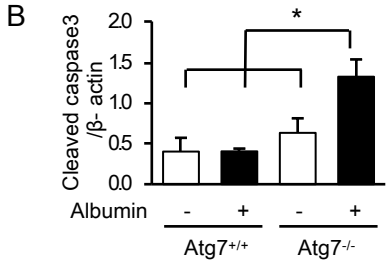

C

rank	Pathological event	score	score(p)	score(v)	score(c)
1	Apoptosis	169.294	1.09E-51	0.157	0.897
2	Endoplasmic Reticulum Stress	93.744	6.03E-29	0.133	0.314
3	Adipogenesis	42.153	2.05E-13	0.084	0.139
4	Necroptosis	38.921	1.92E-12	0.066	0.193
5	Excitotoxicity	29.905	9.95E-10	0.054	0.164
6	Epithelial-Mesenchymal Transition	28.548	2.55E-09	0.06	0.12
7	Cell Cycle	25.668	1.88E-08	0.036	0.286
8	Viral Infection	18.507	2.68E-06	0.042	0.099
9	Drug Transporter	18.235	3.24E-06	0.042	0.096
10	Tight Junction	17.971	3.89E-06	0.042	0.093

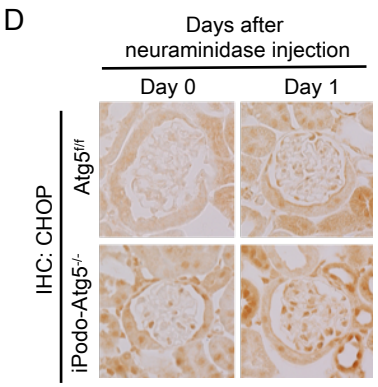

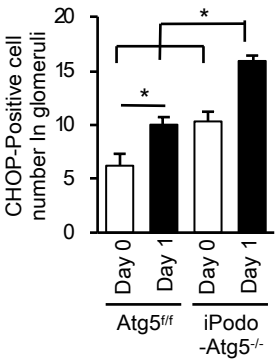

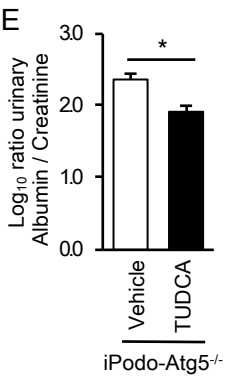

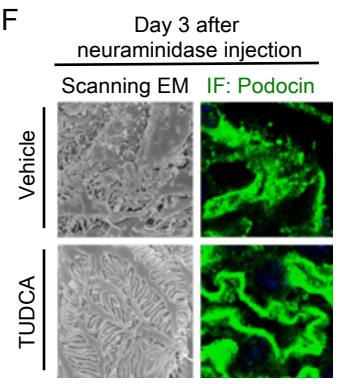

Protective role of podocyte autophagy against glomerular endothelial dysfunction in diabetes

Mamoru Yoshibayashi,[1] Shinji Kume,[1] Mako Yasuda-Yamahara,[1] Kosuke Yamahara,[1] Naoko Takeda,[1] Norihisa Osawa,[1] Masami Chin-Kanasaki,[1] Yuki Nakae,[2] Hideki Yokoi,[3] Masashi Mukoyama,[4] Katsuhiko Asanuma,[5] Hiroshi Maegawa,[1] and Shin-ichi Araki[1]

[1]Department of Medicine, Shiga University of Medical Science, Otsu, Shiga, Japan
[2]Departments of Stem Cell Biology and Regenerative Medicine, Shiga University of Medical Science, Otsu, Shiga, Japan
[3]Department of Nephrology, Graduate School of Medicine, Kyoto University, Kyoto, Japan
[4]Department of Nephrology, Kumamoto University Graduate School of Medical Sciences, Kumamoto, Japan
[5]Department of Nephrology, Graduate School of Medicine, Chiba University, Chiba, Japan.

Supplemental Materials

Supplemental Data. Whole data of the proteomic analysis.

Supplemental Figure 1. Study protocol for high-fat diet (HFD)-induced renal injury in tamoxifen-inducible podocyte-specific Atg5-deficient mice (iPodo-Atg5$^{-/-}$ mice).

Supplemental Figure 2. Spatial interaction between endothelial dysfunction and podocyte dysfunction in high-fat diet (HFD)-fed Atg5$^{f/f}$ and HFD-fed tamoxifen (TM)-inducible podocyte-specific Atg5-deficient mice (iPodo-Atg5$^{-/-}$ mice).

Supplemental Figure 3. No interaction between nitric oxide synthase 3 (NOS3) dysfunction and autophagy deficiency in albuminuria progression of diabetes.

Supplemental Figure 4. Severe podocyte injury in tamoxifen (TM)-inducible podocyte-specific Atg5-deficient mice (iPodo-Atg5$^{-/-}$ mice) with neuraminidase-induced structural endothelial dysfunction.

Supplemental Method.

Supplemental Figure 1

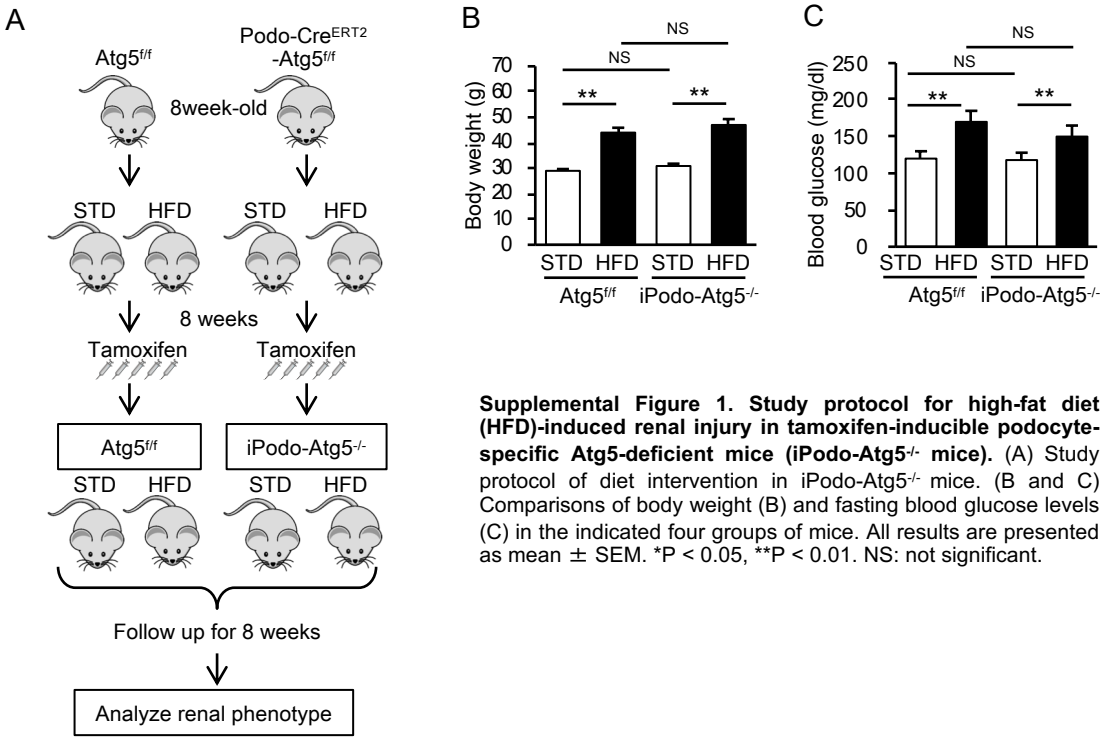

Supplemental Figure 1. Study protocol for high-fat diet (HFD)-induced renal injury in tamoxifen-inducible podocyte-specific Atg5-deficient mice (iPodo-Atg5$^{-/-}$ mice). (A) Study protocol of diet intervention in iPodo-Atg5$^{-/-}$ mice. (B and C) Comparisons of body weight (B) and fasting blood glucose levels (C) in the indicated four groups of mice. All results are presented as mean ± SEM. *P < 0.05, **P < 0.01. NS: not significant.

Supplemental Figure 2

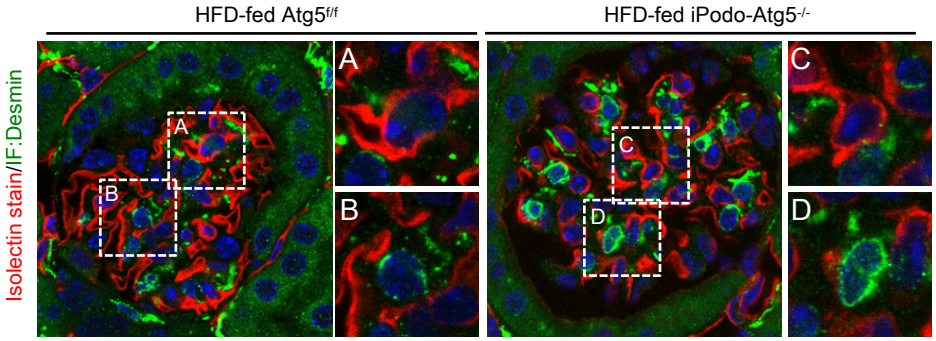

Supplemental Figure 2. Spatial interaction between endothelial dysfunction and podocyte dysfunction in high-fat diet (HFD)-fed Atg5$^{f/f}$ and HFD-fed tamoxifen (TM)-inducible podocyte-specific Atg5-deficient mice (iPodo-Atg5$^{-/-}$ mice). Double immunofluorescent (IF) of desmin and isolectin in glomeruli from the HFD-fed Atg5$^{f/f}$ and HFD-fed iPodo-Atg5$^{-/-}$. Original magnification ×1,000. The white boxes indicate the areas for the magnified pictures (A, B, C, D). The green and red color represents desmin and isolectin, respectively.

Supplemental Figure 3

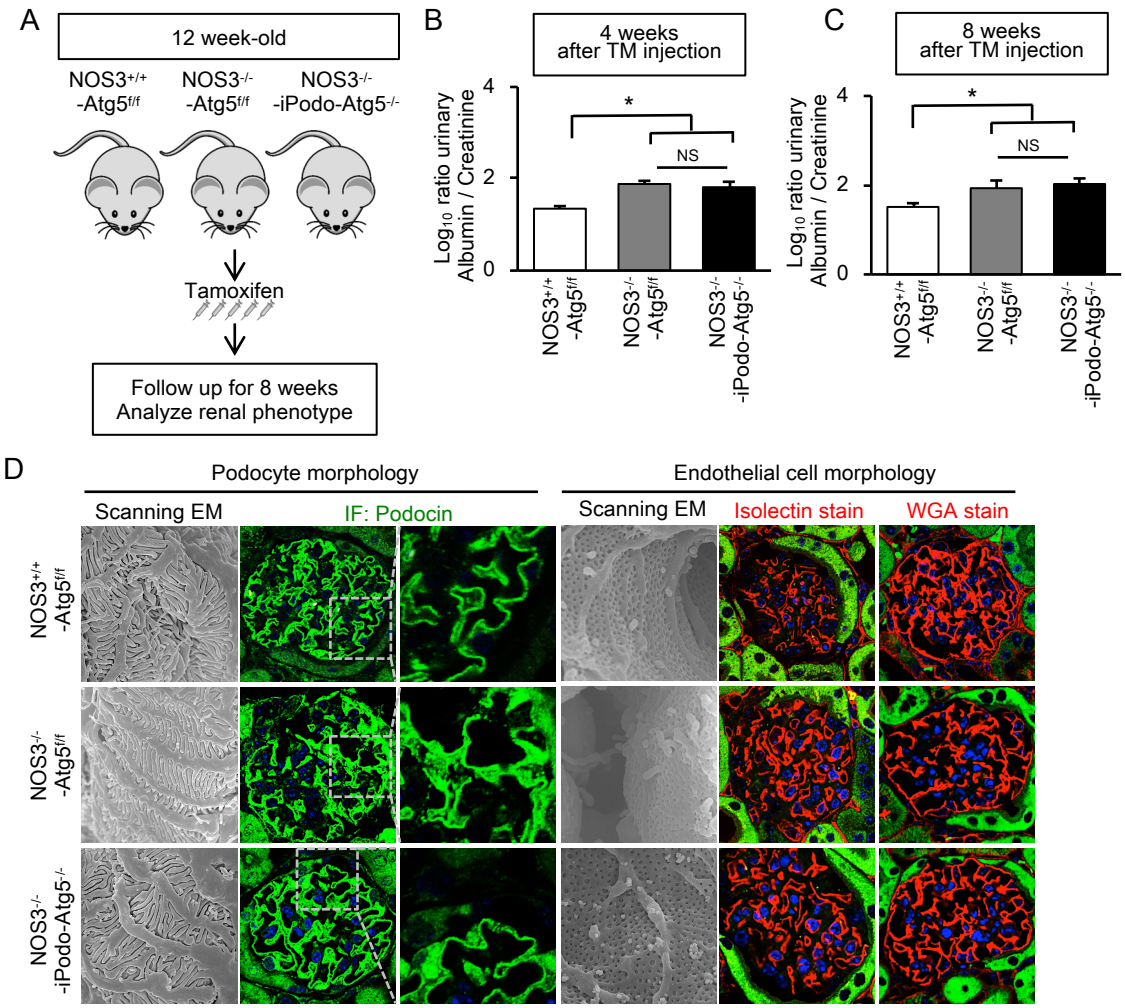

Supplemental Figure 3. No interaction between nitric oxide synthase 3 (NOS3) dysfunction and autophagy deficiency in albuminuria progression of diabetes. We used NOS3-knockout mice as a model with functional endothelial damage. NOS3-deficient mice were purchased from The Jackson Laboratory (Bar Harbor, ME). We crossbred TM-inducible podocyte-specific Atg5-deficient mice with NOS3-knockout mice to produce Atg5 and NOS3-double knockout mice (iPodo-Atg5$^{-/-}$-NOS3$^{-/-}$) (N=5). Age-matched Atg5$^{f/f}$- NOS3-knockout (Atg5$^{f/f}$-NOS3$^{-/-}$) mice were used as a simple NOS3-deficient control (N=5), and age-matched Atg5$^{f/f}$ -NOS3$^{+/+}$were used as a healthy control (N=5). We intraperitoneally injected TM (75 mg/kg/day for 5 consecutive days) into these mice at 12 weeks of age. Urinary samples were collected at 4 and 8 weeks after the TM injection. Mice were sacrificed at 8 weeks after the TM injection.

(A) Protocol for generation of podocyte-specific autophagy-deficient mice with systemic NOS3 deficiency (NOS3$^{-/-}$-iPodo-Atg5$^{-/-}$). (B and C) Urinary albumin excretion levels in NOS3$^{+/+}$-Atg5$^{f/f}$, NOS3$^{-/-}$- Atg5$^{f/f}$, and NOS3$^{-/-}$-iPodo-Atg5$^{-/-}$ mice. Urinary albumin excretion levels are expressed as $\log_{10}$ ratio urinary albumin/ creatinine. (D) Representative images of podocytes and glomerular endothelial cells. Scanning electron microscopy (EM), and immunofluorescence (IF) of podocin, isolectin, and wheat germ agglutinin (WGA). Original magnifications, ×8,000 for scanning EM of podocytes, ×20,000 for scanning EM of glomerular endothelial cells, and ×1,000 for IF of podocin, isolectin, and WGA. The white boxes indicate the areas for the magnified pictures. All results are presented as mean ± SEM. *P < 0.05. NS: not significant

Supplemental Figure 4

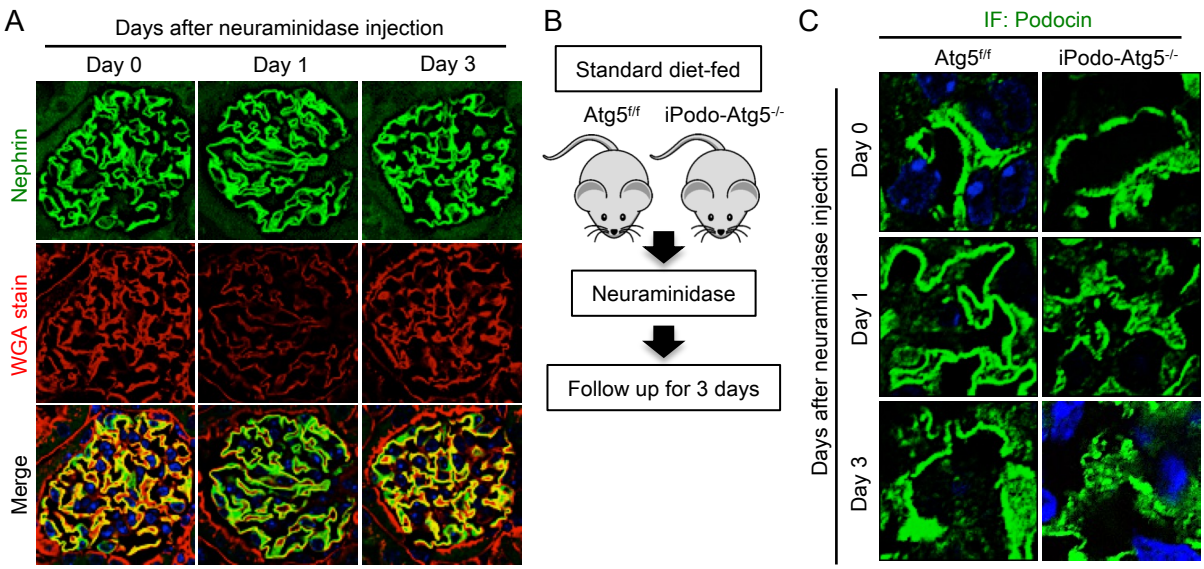

Supplemental Figure 4. Severe podocyte injury in tamoxifen (TM)-inducible podocyte-specific Atg5-deficient mice (iPodo-Atg5$^{-/-}$ mice) with neuraminidase-induced structural endothelial dysfunction. (A) Representative pictures of immunofluorescent (IF) for nephrin and Wheat Germ Agglutinin (WGA). Original magnification: ×1,000. The green and red color represents nephrin and WGA, respectively. (B) Study protocol of neuraminidase-induced structural endothelial dysfunction on standard diet-fed Atg5$^{f/f}$ mice and iPodo-Atg5$^{-/-}$ mice. (C) Immunofluorescent (IF) for podocin. Original magnification: ×1,000 for IF of podocin.

Supplemental Method

HFD-induced diabetic rodent model

Eight-week-old male C57BL/6J mice were obtained from Clea Japan Inc. (Tokyo, Japan). The mice were fed either a STD (10% of total calories from fat) or a HFD (60% of total calories from fat). Mice in STD and HFD groups were sacrificed at 4, 8, 16, and 32 weeks, respectively, after the initiation of dietary intervention.

HFD-induced diabetes in TM-inducible podocyte-specific autophagy-deficient mice

TM-inducible podocyte-specific Atg5-deficient mice (iPodo-Atg5$^{-/-}$) were generated by crossbreeding Atg5$^{f/f}$ mice with TM-inducible Nphs2-Cre transgenic mice (1). Atg5$^{f/f}$ mice were used as a control group. Eight-week-old male Atg5$^{f/f}$ mice were fed the STD or HFD, and eight-week-old male iPodo-Atg5$^{-/-}$ mice were fed the STD or HFD. Each group included 6–12 mice. To induce deletion of the Atg5 gene, we intraperitoneally injected TM (Sigma-Aldrich, St. Louis, MO) at a dose of 75 mg/kg/day for 5 consecutive days into the mice at 8 weeks after the dietary intervention (2). Urinary samples were collected at 4 and 8 weeks after the TM injection. Mice were sacrificed at 8 weeks after the TM injection.

Neuraminidase-induced endothelial damage model

We performed neuraminidase-induced removal of endothelial glycocalyx to establish the structural endothelial damage model (3, 4). Eight-week-old male Atg5$^{f/f}$ mice and iPodo-Atg5$^{-/-}$ mice were injected with neuraminidase via their tail vein at a dose of 0.001 U/gBW (Neuraminidase from *Vibrio cholerae* Type III, Sigma-Aldrich). Urinary samples were collected at the start and following four consecutive days after the neuraminidase injection. Mice were sacrificed at the start of the study and at 1, 3, and 7 days after the neuraminidase injection. The numbers of mice were 3–7 at each time point.

TUDCA treatment of neuraminidase-injected iPodo-Atg5$^{-/-}$ mice

iPodo-Atg5$^{-/-}$ mice were allocated into two groups: vehicle administered, as a control, (N=6) and TUDCA (N=6) groups. TUDCA (500 mg/kg/day, Calbiochem-EMD Millipore, Billerica, MA) was intraperitoneally administered for 3 consecutive days prior to the neuraminidase injection (5). Urinary samples were collected at day 1 after the neuraminidase injection.

Bioinformatic analysis of protein expression data

Pathway analysis of the data list from the proteomic analysis was performed using KeyMolnet (KM Data, Tokyo, Japan) (6). KeyMolnet is a bioinformatics integration platform that enables analysis of specific pathways based on data collected from recent studies. By importing the list of Entrez gene IDs, KeyMolnet automatically provides the corresponding molecules in the form of nodes in a network. Among the various network-searching algorithms, the ‘interaction’ search identifies molecular networks containing a group of molecules with differential regulation in the present study. The significance was scored using the following formula in which O = the number of overlapping molecular relationships between the extracted network and canonical pathway, V = the number of molecules displayed in the search result, C = the number of molecules belonging to specific pathways, T = the total number of molecules recorded in KeyMolnet, and X = the sigma variable that defines incidental agreements.

$$\text{Score(p)} = = \sum_{x=O}^{Min(C,V)} f(X)$$

$$f(X) = {}_{C}C_{X} \bullet {}_{T\text{-}C}C_{V\text{-}X}/{}_{T}C_{V},$$

with Score = $-\log_2$ [Score(p)]; Score(v) = O / V; Score(c) = O / C.

(1) Yokoi, H. *et al.* Podocyte-specific expression of tamoxifen-inducible Cre recombinase in mice. *Nephrol Dial Transplant* **25**, 2120-2124, doi:10.1093/ndt/gfq029 (2010).

(2) Ono, S. *et al.* O-linked β-N-acetylglucosamine modification of proteins is essential for foot process maturation and survival in podocytes. *Nephrol Dial Transplant* **32**, 1477-1487, doi:10.1093/ndt/gfw463 (2017).

(3) Betteridge, K. B. *et al.* Sialic acids regulate microvessel permeability, revealed by novel in vivo studies of endothelial glycocalyx structure and function. *J Physiol* **595**, 5015-5035, doi:10.1113/JP274167 (2017).

(4) Salmon, A. H. *et al.* Loss of the endothelial glycocalyx links albuminuria and vascular dysfunction. *J Am Soc Nephrol* **23**, 1339-1350, doi:10.1681/ASN.2012010017 (2012).

(5) Takeda, N. *et al.* Altered unfolded protein response is implicated in the age-related exacerbation of proteinuria-induced proximal tubular cell damage. *Am J Pathol* **183**, 774-785, doi:10.1016/j.ajpath.2013.05.026 (2013).

(6) Sugahara, S. *et al.* Protein O-GlcNAcylation Is Essential for the Maintenance of Renal Energy Homeostasis and Function. *J Am Soc Nephrol* **30**, 962-978, doi:10.1681/ASN.2018090950 (2019).